



HAL
open science

European climate change at global mean temperature increases of 1.5 and 2 °C above pre-industrial conditions as simulated by the EURO-CORDEX regional climate models

Erik Kjellström, Grigory Nikulin, Gustav Strandberg, Ole Bøssing Christensen, Daniela Jacob, Klaus Keuler, Geert Lenderink, Erik van Meijgaard, Christoph Schär, Samuel Somot, et al.

► To cite this version:

Erik Kjellström, Grigory Nikulin, Gustav Strandberg, Ole Bøssing Christensen, Daniela Jacob, et al.. European climate change at global mean temperature increases of 1.5 and 2 °C above pre-industrial conditions as simulated by the EURO-CORDEX regional climate models. *Earth System Dynamics*, 2018, 9, pp.459-478. 10.5194/esd-9-459-2018 . insu-03721868

HAL Id: insu-03721868

<https://insu.hal.science/insu-03721868>

Submitted on 16 Jul 2022

HAL is a multi-disciplinary open access archive for the deposit and dissemination of scientific research documents, whether they are published or not. The documents may come from teaching and research institutions in France or abroad, or from public or private research centers.

L'archive ouverte pluridisciplinaire **HAL**, est destinée au dépôt et à la diffusion de documents scientifiques de niveau recherche, publiés ou non, émanant des établissements d'enseignement et de recherche français ou étrangers, des laboratoires publics ou privés.



Distributed under a Creative Commons Attribution 4.0 International License



European climate change at global mean temperature increases of 1.5 and 2 °C above pre-industrial conditions as simulated by the EURO-CORDEX regional climate models

Erik Kjellström^{1,2}, Grigory Nikulin¹, Gustav Strandberg¹, Ole Bøssing Christensen³, Daniela Jacob⁴, Klaus Keuler⁵, Geert Lenderink⁶, Erik van Meijgaard⁶, Christoph Schär⁷, Samuel Somot⁸, Silje Lund Sørland⁷, Claas Teichmann⁴, and Robert Vautard⁹

¹Rosby Centre, Swedish Meteorological and Hydrological Institute (SMHI), 601 76 Norrköping, Sweden

²Department of Meteorology (MISU), Stockholm University, 106 91 Stockholm, Sweden

³Danish Climate Centre, Danish Meteorological Institute (DMI), Copenhagen, Denmark

⁴Climate Service Center Germany (GERICS), Helmholtz-Zentrum Geesthacht, Hamburg, Germany

⁵Environmental Meteorology, Brandenburg University of Technology, Cottbus, Germany

⁶Royal Netherlands Meteorological Institute (KNMI), De Bilt, the Netherlands

⁷Institute for Atmospheric and Climate Science, ETH Zürich, Universitätstrasse 16, 8092 Zürich, Switzerland

⁸CNRM UMR 3589, Météo-France/CNRS, Toulouse, France

⁹Laboratoire des Sciences du Climat et de l'Environnement, IPSL, CEA/CNRS//UVSQ, Gif-sur-Yvette, France

Correspondence: Erik Kjellström (erik.kjellstrom@smhi.se)

Received: 31 October 2017 – Discussion started: 17 November 2017

Revised: 12 March 2018 – Accepted: 14 March 2018 – Published: 9 May 2018

Abstract. We investigate European regional climate change for time periods when the global mean temperature has increased by 1.5 and 2 °C compared to pre-industrial conditions. Results are based on regional downscaling of transient climate change simulations for the 21st century with global climate models (GCMs) from the fifth-phase Coupled Model Intercomparison Project (CMIP5). We use an ensemble of EURO-CORDEX high-resolution regional climate model (RCM) simulations undertaken at a computational grid of 12.5 km horizontal resolution covering Europe. The ensemble consists of a range of RCMs that have been used for downscaling different GCMs under the RCP8.5 forcing scenario. The results indicate considerable near-surface warming already at the lower 1.5 °C of warming. Regional warming exceeds that of the global mean in most parts of Europe, being the strongest in the northernmost parts of Europe in winter and in the southernmost parts of Europe together with parts of Scandinavia in summer. Changes in precipitation, which are less robust than the ones in temperature, include increases in the north and decreases in the south with a borderline that migrates from a northerly position in summer to a southerly one in winter. Some of these changes are already seen at 1.5 °C of warming but are larger and more robust at 2 °C. Changes in near-surface wind speed are associated with a large spread among individual ensemble members at both warming levels. Relatively large areas over the North Atlantic and some parts of the continent show decreasing wind speed while some ocean areas in the far north show increasing wind speed. The changes in temperature, precipitation and wind speed are shown to be modified by changes in mean sea level pressure, indicating a strong relationship with the large-scale circulation and its internal variability on decade-long timescales. By comparing to a larger ensemble of CMIP5 GCMs we find that the RCMs can alter the results, leading either to attenuation or amplification of the climate change signal in the underlying GCMs. We find that the RCMs tend to produce less warming and more precipitation (or less drying) in many areas in both winter and summer.

1 Introduction

A main aim of the Paris agreement within the UNFCCC (United Nations Framework Convention on Climate Change) is to keep the increase in the global average temperature well below 2 °C above pre-industrial levels and to pursue efforts to limit the temperature increase to 1.5 °C above pre-industrial levels (UNFCCC, 2015). While the agreement comes into power in 2020 we observe ongoing global warming with the most recent years continuing the long-term warming trend of the last decades (WMO, 2017). Regional and local impacts of global warming are already seen and there is a strong concern that these impacts will become worse with stronger future climate change (IPCC, 2014). However, exactly how strong these impacts will be at different warming levels is uncertain as information about the climate change signal on a regional level is scarce. Despite some efforts that have been made to look at possible climate change at 1.5 or 2 °C of global warming and to compare differences at these global warming levels (e.g. Vautard et al., 2014; Fischer and Knutti, 2015; Schleussner et al., 2016; King and Karoly, 2017), detailed information about regional climate change is largely missing for scenarios reflecting 1.5 °C of global warming (e.g. Mitchell et al., 2016).

Much of the available information about future regional climate change comes from global climate models (GCMs). The most comprehensive set of GCM data is that of the CMIP5 (fifth phase of the Coupled Model Intercomparison Project; e.g. Taylor et al., 2012) consisting of more than 30 GCMs. An advantage with GCMs is that they can provide regional information for all areas in the world. A limitation, however, is the fact that they are commonly operated at relatively coarse horizontal resolution (most often at 100–200 km grid spacing). This implies that land–sea contrasts and land surface properties including mountain height are only described in a coarse way and that important phenomena like mid-latitude cyclones and mesoscale processes are handled in a rudimentary way. Dynamical downscaling with regional climate models (RCMs) is one way of providing high-resolution climate information that better accounts for regional to local scales and thereby adds value compared to the GCM (e.g. Rummukainen, 2010; Sørland et al., 2018). For Europe, relatively large data sets of RCM scenarios have previously been put forward within the context of European research projects including PRUDENCE (Christensen et al., 2007; Déqué et al., 2007) and ENSEMBLES (van der Linden and Mitchell, 2009; Déqué et al., 2012; Kjellström et al., 2013). In recent years RCMs have been operated in the framework of CORDEX (Coordinated Regional Climate Downscaling Experiment; e.g. Jones et al., 2011; Gutowski et al., 2016). For Europe in particular, this means that an unprecedented data set of RCM scenarios at 50 and 12.5 km horizontal resolution is available from the EURO-CORDEX

project (Jacob et al., 2014). Previous works have shown that the high-resolution 12.5 km simulations add value compared to the 50 km simulations, in particular in terms of representing extremes like heavy-precipitation events (e.g. Kotlarski et al., 2014; Prein et al., 2016). Other studies describing evaluation of different important near-surface variables in the EURO-CORDEX RCMs in the recent past climate include those of Smiatek et al. (2016), Knist et al. (2016) and Frei et al. (2018).

The relatively large ensemble of EURO-CORDEX high-resolution RCM climate change scenarios constitutes a valuable data set for impact studies. Some of these simulations and from the earlier ENSEMBLES project have been used for considerations of climate change at different warming levels (e.g. Vautard et al., 2014; Maule et al., 2017) and in impact studies (e.g. Alfieri et al., 2015; Donnelly et al., 2017). However, previous studies have either been based on earlier RCM ensembles or only on smaller subsets of the full EURO-CORDEX set of RCM simulations. In this study we therefore focus on how the European climate may change at the 1.5 or 2 °C of global warming levels in the larger set of EURO-CORDEX simulations at 12.5 km grid spacing. Specifically, we address at which of the two warming levels we can detect significant climate change compared to a reference period in the end of the 20th century and to what extent changes at the two warming levels differ, which is important for mitigation considerations. We also show how different sources of uncertainty influence the climate change signal and discuss how the EURO-CORDEX simulations relate to the larger CMIP5 GCM ensemble.

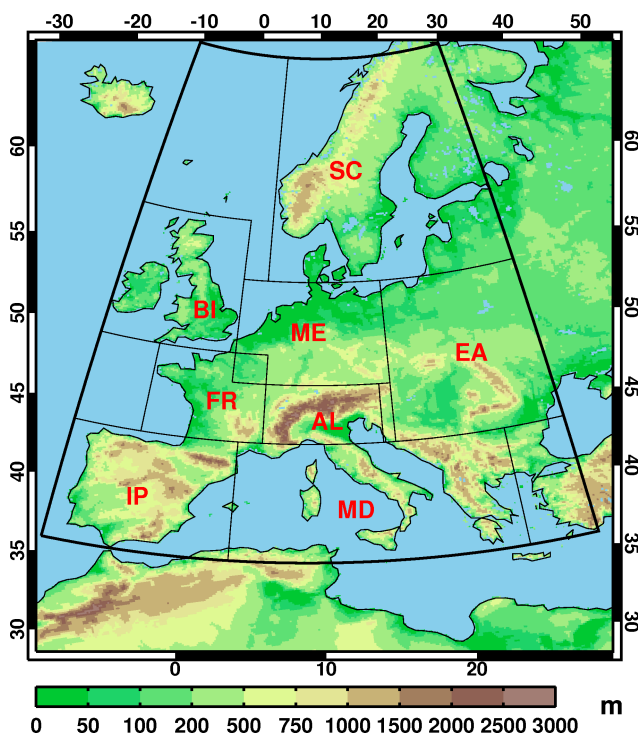
2 Methods and material

2.1 Climate model simulations

We use RCM data from 18 EURO-CORDEX simulations for the European area; see Table 1 and Fig. 1. Specifically, we analyse seasonal mean, 2 m temperature, precipitation, wind speed and mean sea level pressure (MSLP) for all RCMs with the exception of WRF, for which MSLP data are missing. All RCM simulations have been performed with forcing following RCP8.5 (Representative Concentration Pathway; see Moss et al., 2010). The chosen simulations allow us to address the impact of different driving GCMs on the resulting climate change signal. In addition, the impact of the choice of different RCMs can be investigated for both the three-member RCM ensembles downscaling MPI-ESM-LR-r1, EC-Earth-r12, HadGEM2-ES, and CNRM-CM5 and for the two-member ensemble downscaling IPSL-CM5A-MR. Furthermore, as three members of EC-EARTH and two members of MPI-ESM-LR are included, the role of internal natural variability can also be addressed. The simulations have been chosen based on the availability of data at the Earth System Grid Federation (ESGF) facility.

Table 1. Regional climate model simulations assessed in this report. GCMs are listed in more detail in Table 2.

No.	Institute	RCM	GCM	RCM reference
1	SMHI	RCA4	EC-EARTH-r12	Kjellström et al. (2016)
2			HadGEM2-ES	
3			MPI-ESM-LR-r1	
4			CNRM-CM5	
5			IPSL-CM5A-MR	
6	BTU Cottbus	CCLM4-8-17	EC-EARTH_r12	Keuler et al. (2016)
7			CNRM-CM5	
8			MPI-ESM-LR-r1	
9	ETH	CCLM4-8-17	HadGEM2-ES	Keuler et al. (2016)
10	HZG-GERICS	REMO2009	MPI-ESM-LR-r1	Jacob et al. (2012)
11			MPI-ESM-LR-r2	
12	KNMI	RACMO2.2	EC-EARTH-r1	van Meijgaard et al. (2012)
13			EC-EARTH-r12	
14			HadGEM2-ES	
15	DMI	HIRHAM5	EC-EARTH-r3	Christensen et al. (1998)
16			NORESM1-M	
17	CNRM	ALADIN53	CNRM-CM5	Colin et al. (2010); Bador et al. (2017)
18	IPSL	WRF3.3.1	IPSL-CM5A-MR	Skamarock et al. (2008)

**Figure 1.** Map showing the eight subdomains (BI – the British Isles; IP – the Iberian Peninsula; FR – France; ME – mid-Europe; SC – Scandinavia; MD – the Mediterranean region; AL – the Alps; EA – eastern Europe) and the larger European domain for which average climate change signals have been calculated. The colours represent the altitude of the surface in the RCA4 model at the 0.11° EURO-CORDEX grid.

RCM results are set in a larger context by comparing to 31 simulations from the CMIP5 multi-model GCM ensemble (Table 2). In addition to the nine GCM simulations listed in Table 1, the first ensemble members of the other 22 CMIP5 GCMs are also assessed for seasonal mean changes in precipitation and temperature. In this way we can investigate how the smaller subset of GCMs that provides input for the RCMs replicates the larger CMIP5 GCM ensemble. We can also look at if, and to what extent, the RCMs modify the climate change signal compared to that in the underlying GCMs. Comparisons are performed for a number of regions in Europe previously used in a large number of studies (e.g. Rockel and Woth, 2007; Christensen et al., 2010; Kjellström et al., 2013; Keuler et al., 2016), see Fig. 1.

2.2 Calculation of warming levels

We investigate periods for which the global mean near-surface temperature is 1.5 or 2.0 °C above pre-industrial conditions (hereafter referred to as SWL1.5 and SWL2, where SWL stands for specific warming level). As the temperature in true pre-industrial, i.e. pre-1750, conditions are not known (see Hawkins et al., 2017; Schurer et al., 2017), we use the simulated climate from the GCMs for 1861–1890 as a proxy. For each GCM we then identify the first period when the 30-year running mean global temperature reaches 1.5 or 2.0 °C above that of the pre-industrial period. These 30-year time slices (see Table 2) are used for the analyses in the study (see for details Nikulin et al., 2018). For comparing future climate change we then use the period 1971–2000 as our reference in the RCM simulations. This choice is made as (i) the starting point (1971) is the first possible as not all RCMs have data for earlier years and (ii) the end point (2000) is before the

Table 2. CMIP5 GCMs assessed here. Columns SWL1.5 and SWL2 show the central year in a 30-year period when GCMs reach the 1.5 and 2 °C of warming levels (i.e. 2030 represents 2016–2045) under RCP8.5. GCMs are listed in order of when they reach SWL2. Only ensemble member r1 has been used unless otherwise noted in brackets after the GCM name. GCMs in italics have been downscaled by RCMs (see Table 1). For more information see Taylor et al. (2012) and <https://pcmdi.llnl.gov/mips/cmip5/> (last access: 27 April 2018).

No.	Institute	GCM name	SWL 1.5	SWL2
1	Beijing Normal University	BNU-ESM	2009	2023
2	Canadian Centre for Climate Modelling and Analysis	CanESM2	2013	2026
3	Institut Pierre-Simon Laplace	IPSL-CM5A-LR	2011	2027
4	Atmosphere and Ocean Research Institute (The University of Tokyo)	MIROC-ESM	2020	2030
5	National Institute for Environmental Studies, and Japan Agency for Marine-Earth Science and Technology	MIROC-ESM-CHEM	2018	2030
6	National Center for Atmospheric Research	CCSM4	2013	2030
7	<i>Institut Pierre-Simon Laplace</i>	<i>IPSL-CM5A-MR</i>	<i>2016</i>	<i>2030</i>
8	<i>Max Planck Institute for Meteorology</i>	<i>MPI-ESM-LR (r2)</i>	<i>2016</i>	<i>2032</i>
9	NASA/GISS (Goddard Institute for Space Studies)	GISS-E2-H-CC	2017	2035
10	<i>EC-EARTH consortium</i>	<i>EC-EARTH (r1)</i>	<i>2017</i>	<i>2035</i>
11	Geophysical Fluid Dynamics Laboratory	GFDL-CM3	2023	2035
12	<i>Max Planck Institute for Meteorology</i>	<i>MPI-ESM-LR (r2)</i>	<i>2018</i>	<i>2035</i>
13	<i>EC-EARTH consortium</i>	<i>EC-EARTH (r12)</i>	<i>2019</i>	<i>2035</i>
14	NASA/GISS (Goddard Institute for Space Studies)	GISS-E2-H	2020	2036
15	<i>EC-EARTH consortium</i>	<i>EC-EARTH (r3)</i>	<i>2020</i>	<i>2037</i>
16	Institut Pierre-Simon Laplace	IPSL-CM5B-LR	2022	2037
17	<i>Met Office Hadley Centre</i>	<i>HadGEM2-ES</i>	<i>2024</i>	<i>2037</i>
18	Max Planck Institute for Meteorology	MPI-ESM-MR	2020	2038
19	Met Office Hadley Centre	HadGEM2-CC	2029	2041
20	The First Institute of Oceanography, SOA	FIO-ESM	2027	2042
21	<i>Centre National de Recherches Météorologiques/Centre Européen de Recherche et Formation Avancée en Calcul Scientifique</i>	<i>CNRM-CM5</i>	<i>2029</i>	<i>2043</i>
22	Commonwealth Scientific and Industrial Research Organization/Queensland Climate Change Centre of Excellence	CSIRO-Mk3-6-0	2032	2044
23	Met Office Hadley Centre	HadGEM2-AO	2034	2046
24	Norwegian Climate Centre	NorESM1-ME	2032	2046
25	NASA/GISS (Goddard Institute for Space Studies)	GISS-E2-R-CC	2031	2048
26	<i>Norwegian Climate Centre</i>	<i>NorESM1-M</i>	<i>2033</i>	<i>2048</i>
27	Atmosphere and Ocean Research Institute (The University of Tokyo), National Institute for Environmental Studies, and Japan Agency for Marine-Earth Science and Technology	MIROC5	2033	2048
28	NOAA Geophysical Fluid Dynamics Laboratory	GFDL-ESM2M	2034	2051
29	Meteorological Research Institute	MRI-CGCM3	2040	2052
30	Geophysical Fluid Dynamics Laboratory	GFDL-ESM2G	2037	2054
31	Russian Academy of Sciences, Institute of Numerical Mathematics	inmcm4	2043	2058

first year in any of the 30-year SWL1.5 time periods downscaled here (the IPSL model, number 7 in Table 2). From observations we note that the global warming between 1861–1890 (pre-industrial) and 1971–2000 (reference) is 0.41 °C according to HadCRUT4 (Morice et al., 2012), implying that future temperature changes above 1.1 and 1.6 °C represent a regional warming exceeding the global average for the two warming levels.

2.3 Estimation of consistency and robustness of the simulated climate change signal

We calculate differences among 30-year periods as described above and we let the mean over the ensemble members represent the climate change signal for the different variables investigated. Further, we consider the climate change signal to be consistent if at least 80 % of the simulations (14 out of the 18) agree on the sign of climate change. In areas where the climate change signal is found to be consistent we term the change robust if the signal-to-noise ratio is equal to 1 or larger. Here, the signal-to-noise ratio is defined as the ratio between the mean ensemble change divided by 1 SD calcu-

lated over the changes in the individual ensemble members. These characteristics are calculated for both the RCMs and the underlying GCMs.

3 Results

Here we compare simulated changes at SWL1.5 and SWL2 for seasonal mean near-surface temperatures and precipitation and wind speed over Europe for winter (December–February, DJF) and summer (June–August, JJA). We focus on RCM results in the main text; comparable results from the underlying GCMs are given as the Supplement. First, however, we show how changes in MSLP differ among the individual ensemble members as these changes are known to have strong impacts on changes in the other variables (e.g. Van Ulden and van Oldenborgh, 2006; Kjellström et al., 2011; Aalbers et al., 2017).

3.1 Simulated changes in MSLP

Figures 2 and 3 show the changes in MSLP in each ensemble member at SWL2 for winter and summer respectively (apart from WRF for which MSLP data are missing. We have, however, included a blank panel for WRF for consistency with later figures). It is clear that there are considerable differences among the different simulations and that these differences are closely connected to both the choice of GCMs (e.g. comparing CNRM-CM5-driven simulations with those driven by HadGEM2-ES) but also to the choice of ensemble member (as illustrated by the two realizations of MPI-ESM-LR or the three EC-EARTH members). Further, we note that there are some but weaker differences also due to the RCM. The latter can be seen from the six panels showing the RACMO, CCLM and RCA4 simulations downscaling EC-EARTH-r12 and HadGEM2-ES. The most pronounced difference in winter is the stronger increase in MSLP in southern and central Europe in the HadGEM2-ES-driven CCLM simulation compared to the two others (Fig. 2). Also, for summer this CCLM simulation differs compared to the two other RCMs in showing an increase in MSLP in large parts of eastern Europe and the Baltic Sea region (Fig. 3).

In winter we note that the strong north–south pressure gradient over the North Atlantic is changed differently in the different simulations (Fig. 2). In the southern half of the domain in the MPI-ESM-LR-r1-driven simulations there is a weakening in this pressure gradient, while it is intensified in the north. This indicates a northward shift in the storm track with less (more) mild air being advected in over central and southern Europe (northern Scandinavia) from the Atlantic. Similar patterns are seen in the simulations driven by HadGEM2-ES, NorESM1-M and in EC-EARTH-r1. Contrastingly, EC-EARTH-r12 shows a completely different pattern with a strengthening of the north–south pressure gradient, albeit with no major relocation of it, indicating a strengthening of the westerlies over the North Atlantic.

Also, CNRM-CM5 indicates a strengthening of the gradient although not as strong. The MPI-ESM-LR-r2-driven simulation and the EC-EARTH-r3-driven run both show decreasing MSLP over the British Isles and in a band over the European continent, indicating a southward shift of the storm track. Finally, IPSL-CM5A-MR shows a very different pattern with lower pressure in general over large parts of northern Europe, indicating a stronger low-pressure activity in this area.

Also, for summer the change patterns differ. Several simulations indicate a strengthening and/or northward displacement of the subtropical high (the two MPI-ESM-LR members, all EC-EARTH members and NorESM1-M). In MPI-ESM-LR-r1 the strengthened subtropical high is also associated with a decrease in pressure in the northernmost part of the Atlantic and over Scandinavia. This pattern is indicative of a northward shift of the storm track in summer. Five out of the six GCM simulations with a strengthening of the subtropical high show a reinforcement of this signal with warming as the MSLP anomalies are larger at SWL2 than at SWL1.5 (not shown). A similar pattern with reinforcements in MSLP changes when looking at SWL2 compared to SWL1.5 is not generally seen in winter. This contrast between the two seasons indicates that changes in winter are more associated with internal variability while summertime changes are to a larger degree associated with long-term global warming.

3.2 Simulated changes in near-surface temperature

Warming is manifested in all seasons as exemplified for winter and summer in Figs. 4 and 5 (and correspondingly for the underlying GCM ensemble in Figs. S1 and S2). The large-scale features are to a strong degree very similar among the RCMs and the underlying GCMs. A number of regional features stand out from the figures, including a stronger warming in winter than in summer in large parts of northeastern Europe, while the strongest warming in summer is found in the south and southwest but also in parts of Scandinavia. This is consistent with the findings of Vautard et al. (2014), who analysed a different set of simulations and scenarios for the time when global mean temperatures have increased by 2 °C compared to pre-industrial conditions. Changes are generally smaller over the oceans than over land areas, with the exception of some parts of the northern seas that show very strong warming mainly in winter but also to some extent in summer. This strong warming over the northern seas can to a large degree be attributed to reduction in sea ice in the warmer climate. The stronger warming in summer over the Baltic Sea than over its surroundings, however, cannot be directly related to changes in sea ice as there is none in the Baltic Sea in summer. We have not investigated the reason for the Baltic Sea warming in detail here but we note that it is larger in some GCM-driven experiments than others (not shown) so it is likely that the boundary forcing from the GCMs is the cause. A comparison of the climate change signal at the two warming levels shows considerably larger changes at SWL2

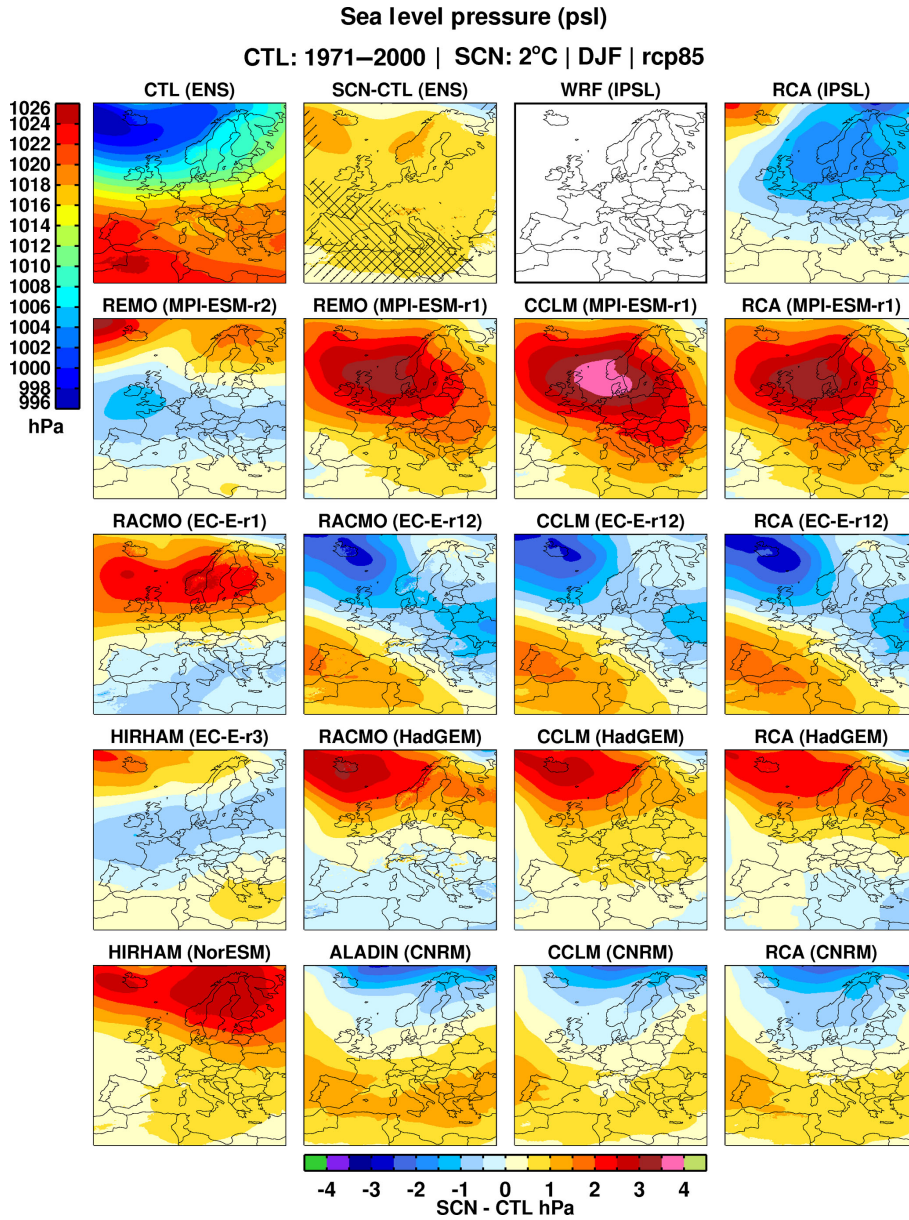


Figure 2. Winter (DJF) mean sea level pressure in the reference period (ensemble mean in the uppermost left panel) and its change in 17 RCM simulations in Table 1 (individual runs in upper right panel and all other rows) for the +2 °C of warming level (SWL2). As MSLP data for the WRF simulation are missing, that panel is left blank. Hatching in the ensemble mean signal (second upper panel from the left) represents areas where at least 14 of the 18 ensemble members agree on the sign of change. Cross-hatching indicates that there is agreement on the sign of change and that the signal-to-noise ratio is larger than 1.

than at SWL1.5. The regional patterns of the differences between the two warming levels closely follow the regional patterns of change outlined above. The results show large areas seeing more than 0.5 °C of additional warming at SWL2. In winter, over northern Scandinavia, additional warming exceeding 1 °C is noted compared to that at SWL1.5 (Fig. 4).

Figures 4 and 5 reveal that temperature increase is a highly consistent feature of the RCM–GCM combinations assessed here as basically all 18 simulations indicate increasing tem-

peratures in both seasons already at SWL1.5. It is only in winter that a few (one to three) ensemble members display a weak decrease at SWL1.5 over parts of eastern Europe and Scandinavia while almost all individual simulations also show warming in all these areas at SWL2 (not shown). Apart from these exceptions over the continent, a few simulations also show the absence of warming over parts of the Atlantic west of the British Isles as a result of a weaker warming in the underlying GCMs in this area. Despite the agreement on

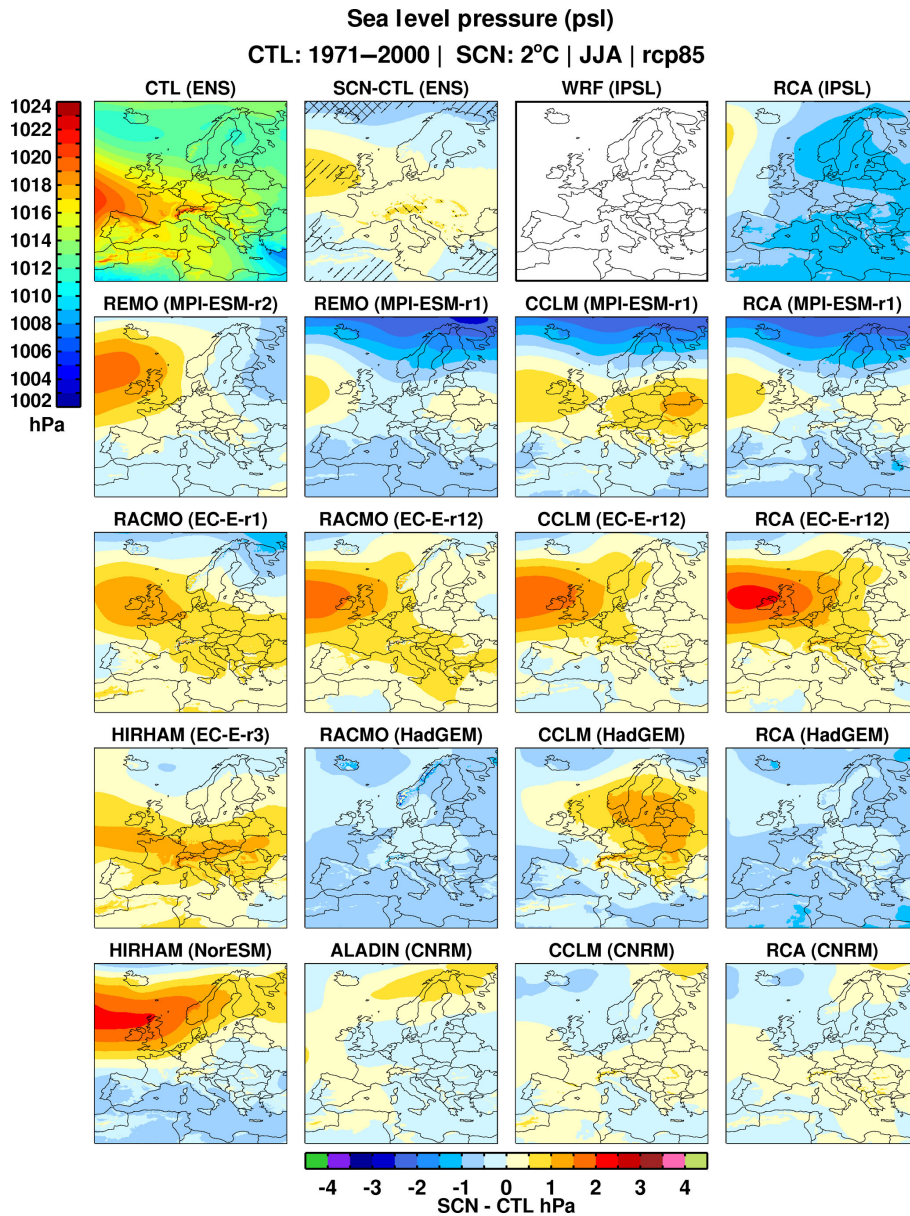


Figure 3. Summer (JJA) mean sea level pressure in the reference period (ensemble mean in the uppermost left panel) and its change in 17 RCM simulations in Table 1 (individual runs in the upper right panel and all other rows) for the +2 °C of warming level (SWL2). Hatching in the ensemble mean signal (second upper panel from the left) represents areas where at least 14 of the 18 ensemble members agree on the sign of change. Cross-hatching indicates that there is agreement on the sign of change and that the signal-to-noise ratio is larger than 1.

sign there are still large differences among individual simulations in some areas (not shown). This is most notable in the far north over ocean areas in winter which is the area in Europe warming the most (see Fig. 4). Apart from the far north we also note relatively large spread in southeastern Europe in winter at both warming levels. A closer look at the individual simulations reveals that the three MPI-ESM-LR-r1-driven simulations all give very modest warming, or even local cooling, for both SWL1.5 and SWL2 (not shown). Recalling the changes in MSLP (Fig. 2) with, on average,

weaker southwesterlies over large parts of the North Atlantic, we interpret this relatively modest warming as a consequence of the changing large-scale circulation bringing less mild Atlantic air in over Europe. Similarly, we can interpret the larger temperature increase in the EC-EARTH-r12-driven RACMO simulation over large parts of Europe compared to the corresponding EC-EARTH-r1-driven one with the changes in MSLP discussed above. Apart from these GCM-driven differences we also note differences arising from choice of RCMs. For instance we note that RCA4

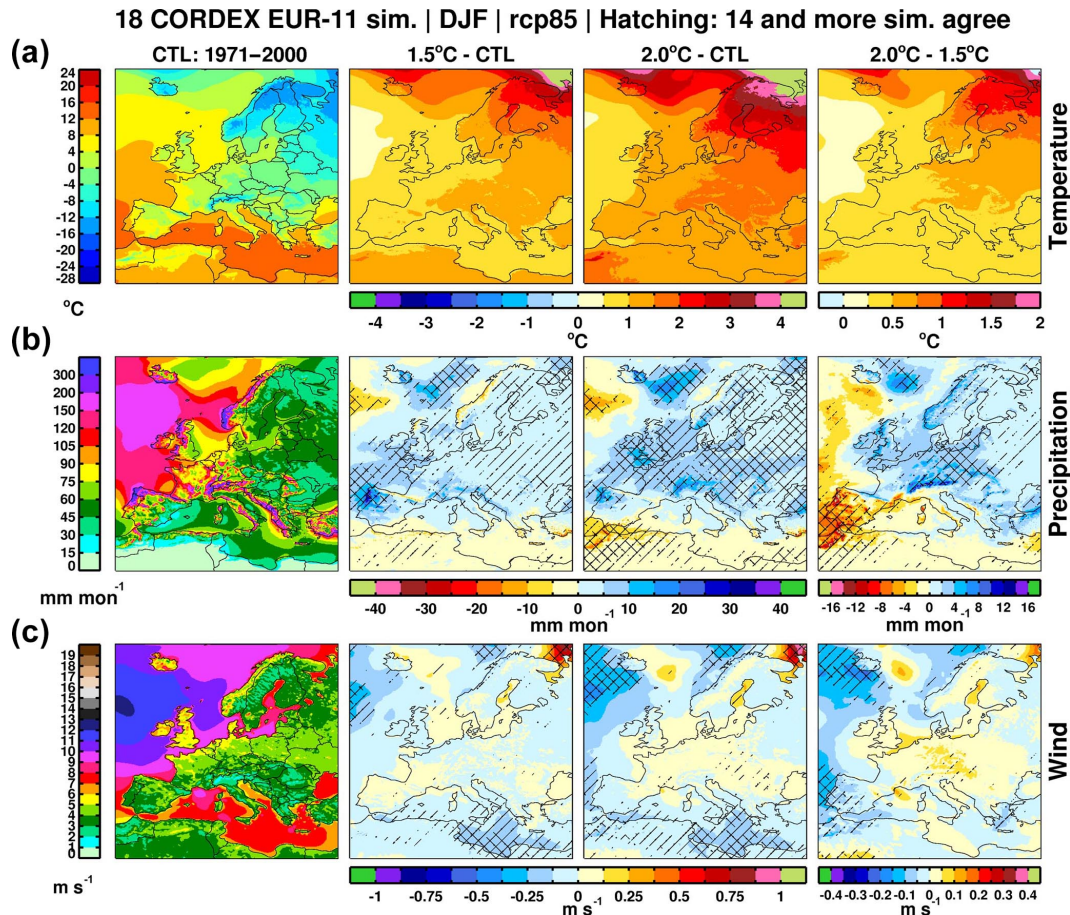


Figure 4. Ensemble mean winter (DJF) 2 m temperature (a), precipitation (b) and 10 m wind speed (c) in the control period (left), its change at SWL1.5 (second column) and SWL2 (third column), and the difference between the change at SWL2 and SWL1.5 (rightmost column). Hatching in the climate change signal for precipitation and wind speed represents areas where at least 14 of the 18 ensemble members agree on the sign of change (for temperature this is always the case). Cross-hatching indicates that there is agreement on the sign of change and that the signal-to-noise ratio is larger than 1. Hatching in the rightmost plots indicates that changes at SWL2 are larger than those at SWL1.5 in at least 14 of the models.

shows stronger warming than CCLM in eastern Europe in winter when forced by EC-EARTH-r12 as does RACMO in the HadGEM2-ESM-driven one (not shown). Similarly, ALADIN shows stronger warming in summer in southeastern Europe than both CCLM and RCA4 when forced by CNRM-CM5. These differences among the RCMs indicate some systematic difference among them and how they respond to changes in the large-scale forcing.

3.3 Simulated changes in precipitation

Precipitation changes in the analysed simulations follow the well-known pattern for Europe, with tendencies for increasing precipitation in the north and decreases in the south on an annual mean basis (not shown). The borderline between increasing and decreasing precipitation migrates from a southerly position in winter (Figs. 4 and S1) to a northerly position in summer (Figs. 5 and S2). As expected, the higher

resolution in the RCMs gives rise to more pronounced differences in coastal and mountainous areas than in the GCMs as the stronger orographic contrasts can amplify the changes. Apart from this, the large-scale features are generally similar in the GCMs and in the RCMs. Changes generally increase over time and the extent of areas showing consistent and robust changes increases from SWL1.5 and SWL2. However, in some areas changes at SWL2 are smaller than those at SWL1.5. As an example the Iberian Peninsula and the adjacent North Atlantic show strong increases in wintertime precipitation already at SWL1.5 while there is no additional increase (or even a weaker signal indicating decrease between the two periods) at SWL2. Compared to the findings for temperature, precipitation changes are less robust. Notably, there are relatively large areas without hatching on the maps where different RCM simulations show either an increase or a decrease in precipitation. We also note that in areas where there is partial consensus of 14–15 models or more on the sign of

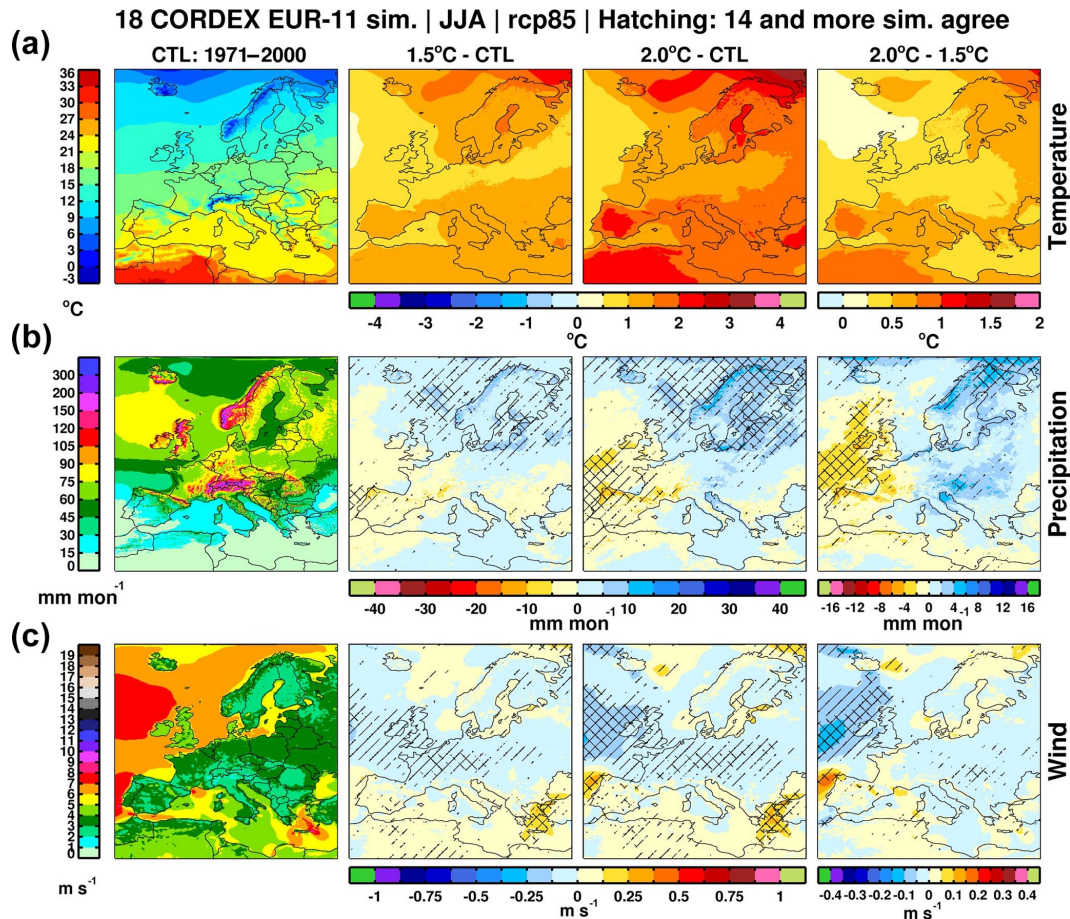


Figure 5. Ensemble mean summer (JJA) 2 m temperature (a), precipitation (b) and 10 m wind speed (c) in the control period (left), its change at SWL1.5 (second column) and SWL2 (third column), and the difference between the change at SWL2 and SWL1.5 (rightmost column). Hatching in the climate change signal for precipitation and wind speed represents areas where at least 14 of the 18 ensemble members agree on the sign of change (for temperature this is always the case). Cross-hatching indicates that there is agreement on the sign of change and that the signal-to-noise ratio is larger than 1. Hatching in the rightmost plots indicates that changes at SWL2 are larger than those at SWL1.5 in at least 14 of the models.

the change there can still be large uncertainties related to the amplitude of the change (Fig. 6).

In some more detail it is clear that some of the differences in precipitation response are strongly related to changes in the large-scale circulation. As an example, a comparison of Figs. 6 and 2 reveals that decreasing precipitation over the North Atlantic south of Iceland in the HadGEM2-ES- and MPI-ESM-r1-driven simulations is connected to higher MSLP and weaker north–south pressure gradients, a pattern that is indicative of weaker westerly winds and less cyclone activity in this area. Contrastingly, the stronger N–S pressure gradient over the Atlantic in the EC-EARTH-r12-driven simulations, and to a lesser extent in the CNRM-CM5-driven simulations, leads to stronger westerlies and substantial increases in precipitation over this region. These regional-scale positive and negative changes in precipitation are more pronounced over parts of the British Isles and southern Norway, which is indicative of orographic amplification of precipita-

tion changes. The northward shift in the storm track in summer (see Fig. 3) is reflected by strong increases in precipitation in parts of Scandinavia (Fig. 5). In southern and central Europe, however, there is a reduction in precipitation in connection with the northward displacement of the subtropical high and increasing MSLP over Europe. Again, there are also large differences among individual RCMs when forced by the same driving GCM simulation. Examples include stronger increases in precipitation in RCA4 compared to CCLM and RACMO in northern Scandinavia (not shown).

3.4 Simulated changes in near-surface wind speed

The simulated climate change signal in mean near-surface wind speed is generally not consistent over Europe. Decreases are seen over parts of the North Atlantic and the Mediterranean in winter (Figs. 4 and S1) and over parts of the North Atlantic and western Europe in summer (Figs. 5

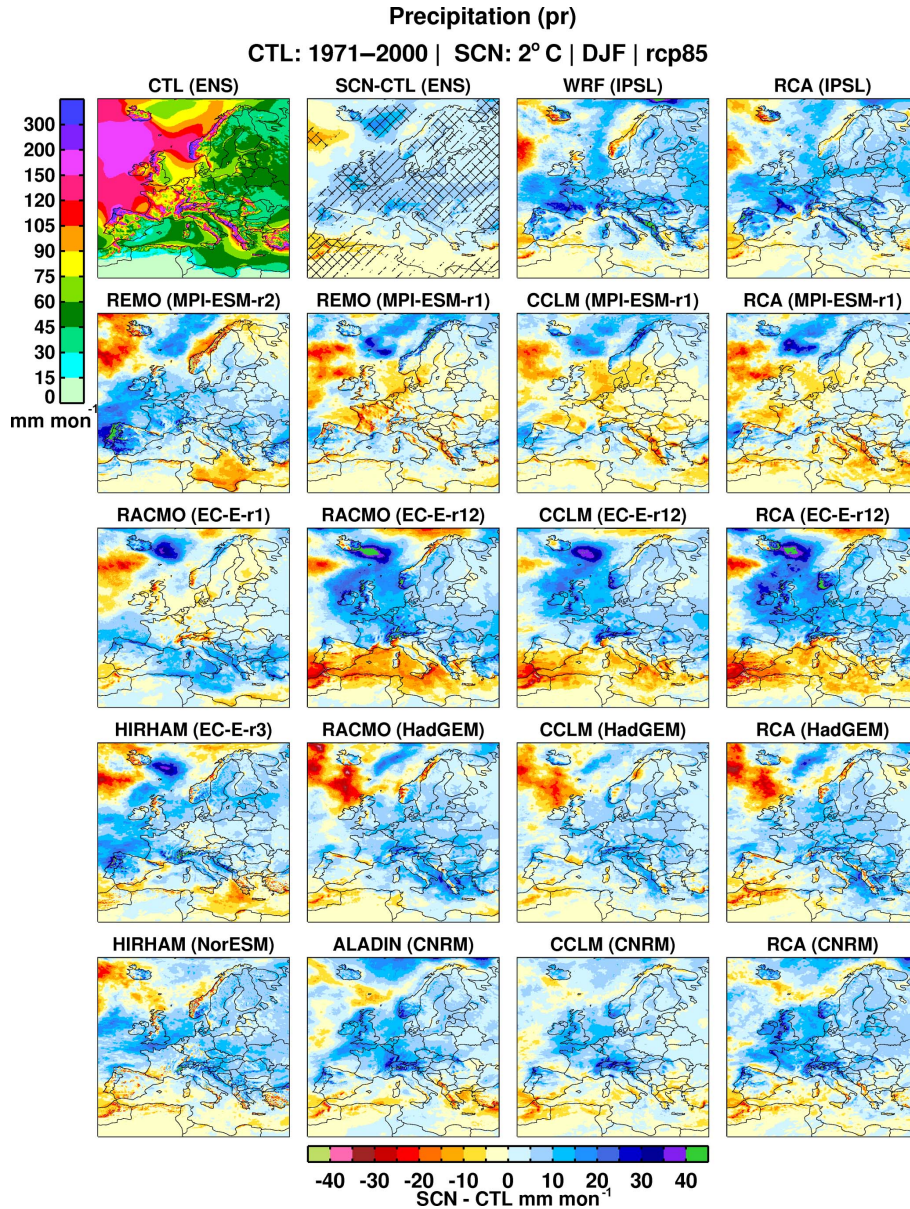


Figure 6. Winter (DJF) precipitation in the reference period (ensemble mean in the uppermost left panel) and its change in 18 RCM simulations in Table 1 (two uppermost right panels and all other rows) for the +2 °C of warming level (SWL2). Hatching in the ensemble mean signal (second upper panel from the left) represents areas where at least 14 of the 18 ensemble members agree on the sign of change. Cross-hatching indicates that there is agreement on the sign of change and that the signal-to-noise ratio is larger than 1.

and S2), confirming the results of Tobin et al. (2016). Increases are seen over some northern ocean areas, most notably in the RCMs but to some extent also in the GCMs. These are strongest in winter but can to some extent be seen in all seasons. A closer look at the individual simulations reveals that there are strong connections to the variability in the large-scale circulation as indicated by changes in the MSLP pattern. Notably, the weakening and northward shift in the N–S pressure gradient in the HadGEM2-ES-driven simulations is reflected in a considerable decrease in wind speed

in large parts of the area, while the sharpening of the gradient in the EC-EARTH-r12-driven simulations leads to strong increases in wind speed in the area of the British Isles (compare Figs. 2 and 7). Apart from these changes that are related to changes in the large-scale circulation, there are also other wind speed changes. Figure 7 reveals that the local increases over parts of the northern oceans are seen in most simulations although at slightly different locations. There are no common changes in MSLP that can explain this pattern. However, we note strong increases in near-surface temperature in

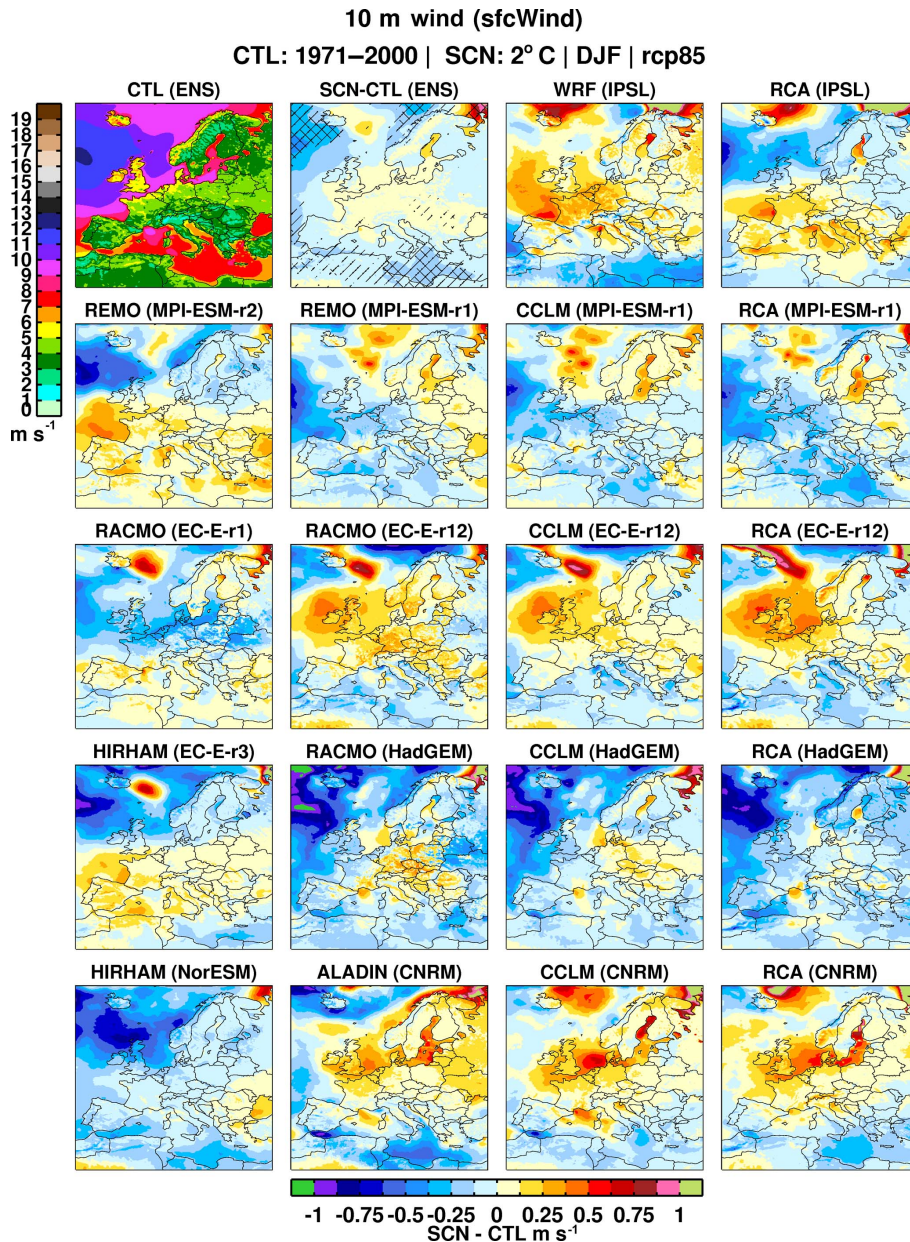


Figure 7. Winter (DJF) 10 m wind speed in the reference period (ensemble mean in the uppermost left panel) and its change in 18 RCM simulations in Table 1 (two uppermost right panels and all other rows) for the +2 °C of warming level (SWL2). Hatching in the ensemble mean signal (second upper panel from the left) represents areas where at least 14 of the 18 ensemble members agree on the sign of change. Cross-hatching indicates that there is agreement on the sign of change and that the signal-to-noise ratio is larger than 1.

these areas in the models (not shown). This strong relation between near-surface temperature and winds indicates that changing surface conditions are important here. The reduction of sea ice and the associated higher temperatures likely lead to a less stably stratified planetary boundary layer that thereby becomes more favourable for downward mixing of momentum leading to higher wind speed close to the surface. Also in summer, changes in sea ice and associated changes in sea surface temperatures (SSTs) may contribute to increasing

wind speed over the Arctic Ocean areas in some simulations (not shown). However, we also note similar differences in some simulations over the Baltic Sea where sea ice cannot be the reason for summertime differences. Changes in wind speed are more pronounced in some areas at SWL2 than at SWL1.5, indicating that we are looking at a manifestation of long-term climate change. However, we note that the areas where models agree upon sign of change in wind speed do not become considerably larger at SWL2 and that large areas

do not show any systematic changes in wind speed reflecting the importance of internal variability. In summary, the results indicate that it is highly uncertain what may happen to wind speed in this region when global warming continues.

4 Discussion

4.1 Is there a detectable climate change signal in the EURO-CORDEX ensemble at 1.5 and 2 °C of global warming?

The results of the 18 RCM simulations analysed here show increasing temperatures, changing precipitation patterns and also some changes in seasonal mean wind speed (Figs. 4 and 5). These changes are more or less consistent and robust for the different variables. The ensemble mean shows consistent and robust changes in all land areas already at SWL1.5 for both seasons (Table 3), and temperature increases are simulated in all parts of Europe for all seasons by all individual models (not shown). Differences between SWL1.5 and SWL2 amount to somewhere between 0.3 and 0.8 °C for summer and winter seasonal mean conditions averaged over the different regions in Fig. 1 (compare Table 4 and S1). Precipitation changes show larger model spread, and ensemble mean changes at SWL1.5 are consistent and robust in only less than 10 % of the European land areas (Table 3). Despite generally larger changes, this fraction is also relatively small at SWL2 and it is not until higher warming levels (2.5 and 3 °C above pre-industrial conditions) that the ensemble mean signal is consistent and robust in more than half of Europe for winter. For summer this still only applies for less than 25 % of the European land areas even at 3 °C of warming. This low degree of consistency and robustness reflects the uncertainties even in sign of change in the seasonally migrating area between increasing precipitation in the north and decreasing precipitation in the south. For wind speed there are also large uncertainties with different models showing very different response patterns, and the fraction of Europe for which there is a consistent and robust change is as low as that for precipitation in summer, while in winter it is even less (Table 3). We note that for the studied variables the ensemble mean changes at SWL2 are generally larger than those at SWL1.5. This is always the case for temperature, while for precipitation and wind speed there are local exceptions to this. Differences among individual ensemble members are often large, sometimes larger than the overall climate change signal at SWL1.5 and SWL2. It is evident that while a clear robust climate change signal is seen for temperature it has not emerged in all other variables, seasons and regions studied here. This finding is in accordance with earlier studies that have also shown different times of emergence of a regional climate change signal (e.g. Giorgi and Bi, 2009; Hawkins and Sutton, 2012; Kjellström et al., 2013). Table 3 reveals that at even higher warming levels SWL2.5 and SWL3 the fraction of land with consistent and robust changes also increases

for these variables, but there are still large areas where such changes are not evident.

The results indicate that the large-scale circulation has an important role in determining the actual climate change signal in any individual simulation. For instance, it is clear that stronger westerlies in some simulations are associated with milder and wetter conditions over parts of the continent while weaker westerlies are associated with less precipitation along the western coastlines. This is in concert with previous studies showing a similar dependence (e.g. Van Ulden and van Oldenborgh, 2006; Kjellström et al., 2011; Kjellström et al., 2013). Differences in the large-scale circulation over decade-long climate simulations are not necessarily a sign of climate change but rather a manifestation of the large internal variability in the climate system that can be pronounced on a regional scale (e.g. Hawkins and Sutton, 2009). As our results are based on a relatively small number of GCM simulations we are limited in the degree to which the ensemble captures the full uncertainty. Larger ensembles consisting of multiple simulations with one, or preferably many models, would provide a better opportunity to sample this uncertainty (e.g. Deser et al., 2012; Aalbers et al., 2017). It is clear that the natural variability with its impacts on the large-scale circulation is a major cause of uncertainty. This is highly pronounced when it comes to assessing climate change signals at any of the two warming levels discussed here as changes still do not, even if robust and seen in most simulations, necessarily exceed the natural variability.

4.2 Timing for reaching 1.5 and 2 °C above pre-industrial conditions

An alternative approach to the one used here for investigating climate change at the time of 1.5 and 2 °C of warming would be to use scenarios in which the climate system reaches a new equilibrium at the requested warming levels. This could for instance be closer to the end of the century in scenarios with rapidly decreasing forcing and eventual stabilization of the climate. A difficulty with that approach is that different GCMs with different climate sensitivities may either not reach the warming levels or exceed them. The definition of warming levels used here assures that the global mean warming for the investigated periods is exactly 1.5 and 2 °C above pre-industrial conditions as simulated by the models. The choice of extracting this information from a transient simulation implies that there will be trends in the time slices that may influence the results (Bärring and Strandberg, 2018). For instance, interannual variability may be artificially augmented in case of a long-term increasing (or decreasing) trend. Such trends could be removed before investigating interannual variability or extreme conditions that may be sensitive to increased temporal variability. However, for this study we have chosen not to do this as we focus on long-term seasonal averages. Another potential problem with the transient approach is when results are going to be used in impact stud-

Table 3. Summary statistics showing the fraction of land in the larger European domain (see Fig. 1) where the ensemble members show consistent changes (80 % agree on sign) and in addition show a robust change for four different warming levels between 1.5 and 3 °C as defined in Sect. 2.3. The numbers in parentheses represent the corresponding fraction from the underlying GCM ensemble.

		1.5 °C	2 °C	2.5 °C	3 °C
Winter (DJF)					
Temperature	Consistent	100 (100)	100 (100)	100 (100)	100 (100)
	Consistent and robust	100 (100)	100 (100)	100 (100)	100 (100)
Precipitation	Consistent	47 (45)	67 (75)	75 (80)	79 (87)
	Consistent and robust	9 (11)	40 (32)	64 (63)	67 (82)
Wind speed	Consistent	7 (40)	10 (30)	14 (29)	13 (50)
	Consistent and robust	0 (15)	1 (11)	3 (9)	3 (18)
Summer (JJA)					
Temperature	Consistent	100 (100)	100 (100)	100 (100)	100 (100)
	Consistent and robust	100 (100)	100 (100)	100 (100)	100 (100)
Precipitation	Consistent	24 (40)	37 (47)	44 (50)	53 (58)
	Consistent and robust	4 (18)	15 (25)	18 (35)	25 (39)
Wind speed	Consistent	32 (25)	45 (45)	51 (42)	52 (54)
	Consistent and robust	7 (1)	14 (9)	25 (15)	27 (28)

ies for which there may be other important time constraints. A certain level of global climate change may have very different regional signatures at different timings. For instance, Maule et al. (2017) shows that if the time it takes until a certain warming level is reached is longer (as a result of weaker forcing in RCP4.5), the regional climate change signal in Europe is weaker than if the level is reached quickly (as result of strong forcing in RCP8.5). Apart from such differences in regional climate response, impacts will be different if changes are quick or slow depending on the resilience of the considered society or ecosystem.

Here, we present information about when the two specific warming levels are reached given the data used in the study. A benefit of this transient, non-stabilized approach is that it represents conditions that may be more representative for what happens if we do not meet the 2 °C target (or 1.5 °C for that matter). Even if global warming will be more than 2 °C it may be valuable to look at SWLs in an adaptation context, as a level of climate change that we will have to adapt to on our way to the even warmer climate beyond 2 °C. In that case this approach is a way to shift the perspective from the relatively uncertain level of climate change at a specific point in time to a more certain level of climate change at an uncertain point in time.

Partly due to their different climate sensitivity the CMIP5 GCMs reach the different warming levels at different points in time. For the 31 RCP8.5 runs in Table 1 the central years of the 30-year periods range between 2009 and 2043. The subset of GCMs that has been downscaled in EURO-CORDEX and further assessed here shows central years ranging between 2016 and 2029. Therefore, it is clear that the chosen subset does not sample the full range of climate sensitivities in the GCMs.

Some GCMs have been run several times to sample the natural variability in the system and usually these ensemble members show slightly different results. The largest ensemble of one GCM in the CMIP5 data set is the CSIRO model with 10 different members (member number 1 is shown in Table 2). The central year for reaching the 1.5 °C of warming level in that 10-member ensemble ranges between 2027 and 2035. For the corresponding 2 °C level it ranges between 2041 and 2046. These relatively smaller intervals, compared to those of the CMIP5 multi-model ensemble discussed above, indicate that the simulated natural variability in the global mean temperature is a smaller source of uncertainty than that of the climate sensitivities as represented by the different GCMs. This does not, however, imply that natural variability on the regional scale is not important as a source of uncertainty (as discussed in Sect. 4.1).

In addition to climate model sensitivity and natural variability, different forcing also plays a role in when a certain warming level is reached. We note that the 30-year time slices used in the analysis here partly overlap between the two time windows. For the RCP8.5 scenarios central years between the two periods differ by between 18 and 10 years in any of the GCM simulations, indicating that at least 12 years is common for the two time slices for any given simulation while for some model simulations a variation of even up to 20 years is the same. Clearly, the two samples are more similar compared to if they were taken as time slices more separated from each other. This similarity has implications for how to assess differences between the periods in a statistically rigorous way as data in the two samples are not independent.

All 31 GCMs in Table 2 have also been run for RCP4.5. For that scenario SWL1.5 is reached between 2008 and 2061 in the different models (not shown). SWL2, however, is

Table 4. Summary statistics showing temperature and precipitation changes at SWL1.5 for the eight regions in Fig. 1. For each region there are three sets of data for each season and variable representing the full CMIP5 ensemble (top), the nine-member GCM ensemble downscaled by the RCMs (middle) and the 18-member RCM ensemble (lower). The numbers represent the minimum (left), maximum (right) and mean plus or minus 1 SD (middle) of the ensemble members' individual area mean climate changes.

Area	Near-surface temperature (°C)						Precipitation (%)					
	DJF			JJA			DJF			JJA		
	Min	Mean ± SD	Max	Min	Mean ± SD	Max	Min	Mean ± SD	Max	Min	Mean ± SD	Max
IP	0.35	0.92 ± 0.35	1.67	0.58	1.42 ± 0.55	2.68	−17	−2.0 ± 8.9	19	−33	−7.8 ± 8.6	13
	0.40	0.87 ± 0.40	1.67	0.74	1.16 ± 0.47	1.99	−3.6	5.6 ± 6.8	19	−21	−7.3 ± 8.6	9.4
	0.35	0.79 ± 0.40	1.58	0.58	0.94 ± 0.32	1.59	−2.7	3.5 ± 5.3	19	−16	−6.0 ± 5.3	3.9
MD	0.37	1.02 ± 0.44	1.95	0.65	1.54 ± 0.59	2.75	−19	−3.0 ± 6.8	10	−30	−6.3 ± 9.8	15
	0.37	0.94 ± 0.44	1.75	0.72	1.36 ± 0.54	2.30	−8.1	1.4 ± 6.4	10	−28	−11 ± 8.1	−1.5
	0.27	0.92 ± 0.43	1.77	0.66	1.16 ± 0.36	1.85	−7.7	1.0 ± 5.6	12	−18	−1.7 ± 9.0	15
FR	0.44	1.01 ± 0.44	2.04	0.23	1.33 ± 0.63	2.65	−13	3.4 ± 5.8	13	−27	−5.3 ± 9.5	15
	0.46	0.84 ± 0.41	1.63	0.44	1.05 ± 0.59	2.13	−9.1	3.6 ± 6.8	11	−12	−5.1 ± 7.4	12
	0.25	0.83 ± 0.41	1.46	0.51	0.90 ± 0.33	1.81	−6.7	4.5 ± 6.0	12	−11	−2.0 ± 7.7	11
AL	0.28	1.29 ± 0.64	2.91	0.51	1.65 ± 0.74	3.43	−11	3.6 ± 7.6	16	−29	−1.3 ± 9.2	26
	0.40	1.12 ± 0.69	2.59	0.54	1.45 ± 0.69	2.63	−3.6	5.4 ± 7.1	15	−8.6	−1.7 ± 4.6	4.8
	0.24	1.07 ± 0.53	2.00	0.73	1.15 ± 0.30	1.86	−6.8	5.2 ± 5.5	12	−13	−0.5 ± 6.6	10
EA	−0.23	1.49 ± 0.77	3.54	0.45	1.76 ± 0.87	4.02	−12	4.8 ± 5.6	14	−23	0.3 ± 9.3	16
	−0.23	1.21 ± 0.77	2.30	0.51	1.53 ± 0.85	3.26	−12	4.4 ± 7.3	11	−16	0.2 ± 9.5	16
	−0.21	1.14 ± 0.74	2.07	0.40	1.09 ± 0.44	1.83	−8.6	6.0 ± 6.6	13	−7.5	2.1 ± 4.6	11
BI	0.09	0.81 ± 0.36	1.75	−0.15	0.97 ± 0.52	1.97	−2.0	4.7 ± 4.6	17	−16	−1.1 ± 7.0	16
	0.09	0.70 ± 0.32	1.06	0.39	0.83 ± 0.45	1.80	−2.0	2.7 ± 4.0	9.5	−12	0.0 ± 7.7	12
	0.11	0.71 ± 0.28	1.02	0.35	0.83 ± 0.34	1.60	−4.8	3.5 ± 4.4	11	−5.4	1.0 ± 4.7	7.4
ME	0.14	1.24 ± 0.56	2.71	0.08	1.41 ± 0.73	3.27	−13	6.4 ± 6.1	15	−18	0.9 ± 9.8	23
	0.14	0.98 ± 0.54	1.85	0.35	1.14 ± 0.70	2.59	−13	3.3 ± 7.8	12	−6.8	2.6 ± 8.9	21
	0.08	0.94 ± 0.51	1.67	0.40	1.00 ± 0.37	1.85	−11	4.3 ± 7.6	13	−8.6	1.5 ± 5.6	11
SC	−0.06	1.67 ± 0.71	3.10	0.16	1.45 ± 0.66	2.83	−4.0	5.4 ± 4.8	16	−4.7	4.2 ± 5.5	13
	0.23	1.42 ± 0.55	2.10	0.35	1.25 ± 0.66	2.50	−4.0	1.6 ± 3.3	5.3	−3.9	5.8 ± 5.9	13
	0.22	1.53 ± 0.44	2.00	0.52	1.25 ± 0.51	2.20	−5.4	3.2 ± 3.3	6.8	−1.1	5.3 ± 3.1	10

reached at 2024 by the first model, while for five of the models it is not reached at all during the 21st century. For the 26 simulations that do reach SWL2 under RCP4.5 the timing for any one of them differs from the time when the same simulation reaches SWL1.5 by between 35 and 14 years, indicating that in some cases there is no overlap between the two warming levels but in some cases up to 16 years is common. Clearly, there is an impact on the similarity of the results between the two time slices depending on which scenario that is used.

4.3 How representative are the results from the EURO-CORDEX ensemble?

In this section we discuss how the above-mentioned RCM-based results relate to the underlying GCMs and to the larger CMIP5 ensemble by showing scatter plots for changes in temperature and precipitation. We present scatter plots for

Scandinavia and eastern Europe as these are the two areas in Fig. 1, which shows the strongest changes in temperature: in winter in Scandinavia and in summer in eastern Europe. Precipitation shows an increase in Scandinavia in both winter and summer. In eastern Europe it increases in winter while different models show either increases or decreases in summer. Comparing and contrasting these areas gives a good picture of changes in some of the climate regimes of Europe. In Table 4 we present summary statistics for SWL1.5 in the sub-regions defined in Fig. 1.

Figure 8 and Table 4 show that simulated temperature changes in Scandinavia are larger in winter (1.7 °C) than in summer (1.5 °C). For comparison with pre-industrial conditions we remind ourselves that this change is to be added to the 0.41 °C increase in global mean temperature between 1861–1890 and 1971–2000. For the Scandinavian region past changes are larger; data representing Sweden show that warming over this period is almost 1 °C (data taken

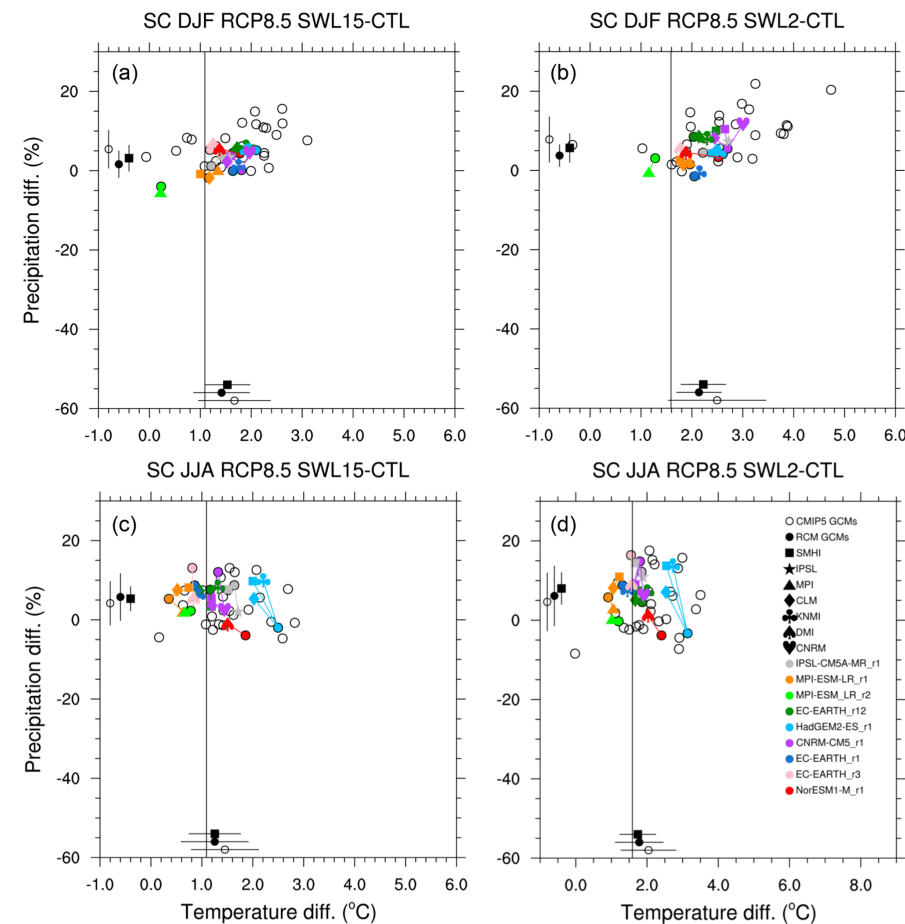


Figure 8. Temperature and precipitation changes over Scandinavia (SC, Fig. 1) for winter (a, b) and summer (c, d) mean conditions. Panels (a, c) show SWL1.5 and (b, d) SWL2. The error bars plotted inside the axis in the diagram illustrate the average and plus or minus 1 SD from (i) the CMIP5 ensemble (Table 2), (ii) the nine-member GCM ensemble that has been downscaled and (iii) the 18-member RCM ensemble (Table 1). Unfilled circles are CMIP5 GCMs listed in Table 2 that have not been downscaled. Filled circles represent GCMs that have been downscaled and these are connected by a line to the RCM(s) that have been used for downscaling. The vertical line represents the global mean warming at SWL1.5 and SWL2 relative to the control period (1971–2000).

from www.smhi.se, last access: 10 March 2018), indicating a warming of more than 2.5 °C compared to pre-industrial conditions already at SWL1.5. Figure 8 shows that the simulated future warming is stronger in Scandinavia compared to the global mean warming already at SWL1.5 and even more pronounced at SWL2 for the majority of the simulations. For precipitation, the majority of the simulations indicate that it will become wetter in both winter and summer, which is already seen at SWL1.5 and more clearly in SWL2 in many simulations. However, for both seasons there are also simulations showing only little change or even decreasing precipitation.

It is clear that the spread among the simulations becomes larger at SWL2 compared to SWL1.5 in both temperature and precipitation based on the full CMIP5 model ensemble. We note that the RCM-simulated changes in temperature and precipitation mostly lie within the range of those as

simulated by the underlying GCMs and by the larger CMIP5 ensemble. However, it is also clear that the range spanned by the RCM ensemble (or that spanned by the underlying GCMs) is more limited compared to the full CMIP5 ensemble. Comparing individual simulations reveals that the RCMs do modify the climate change signal from the underlying GCMs. There are, however, large differences in how large these modifications are. For instance, the REMO RCM only changes the climate change signal from the MPI-ESM-LR model marginally in all four cases while all three RCMs that have downscaled HadGEM2-ES change the results significantly in summer. In the latter case it is even the question of changing sign in the precipitation signal: from a decrease in HadGEM2-ES to an increase in the RCMs. A similar discrepancy between HadGEM2-ES and RCA4 was also found in an RCA4 simulation at 50 km horizontal resolution by Kjellström et al. (2016). They also found wetter condi-

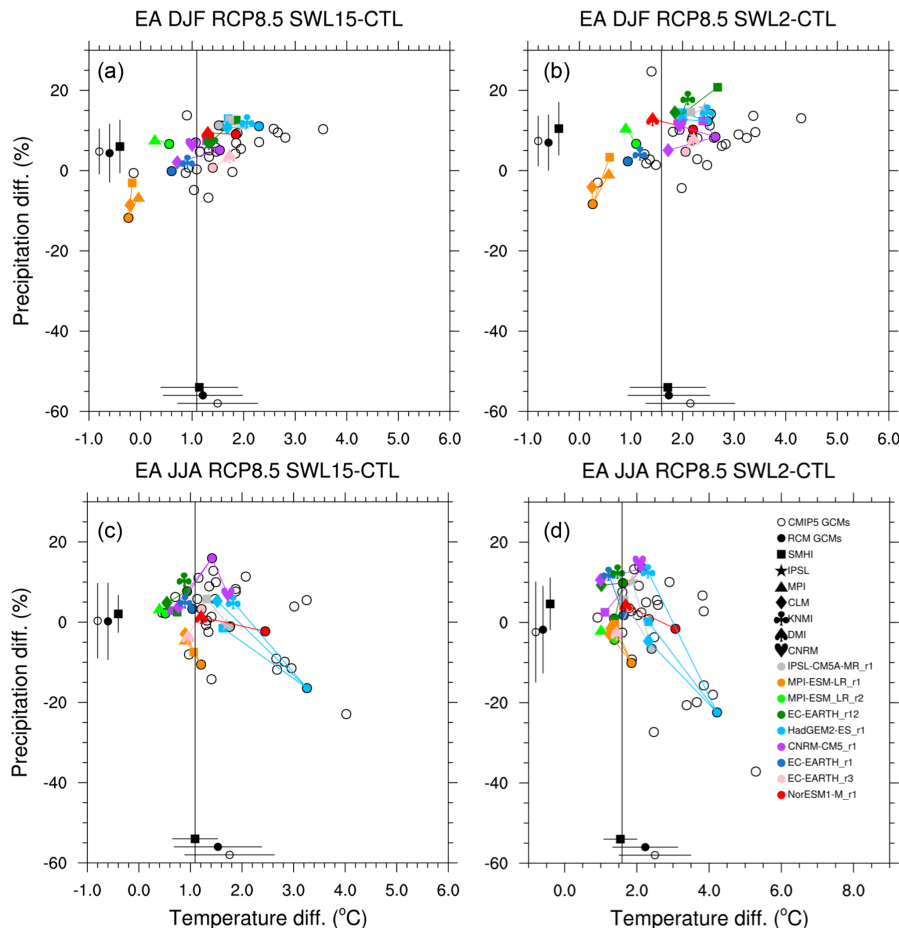


Figure 9. Temperature and precipitation changes over eastern Europe (EA, Fig. 1) for winter (a, b) and summer (c, d) mean conditions. Panels (a, c) show SWL1.5 and (b, d) SWL2. The error bars plotted inside the axis in the diagram illustrate the average and plus or minus 1 SD from (i) the CMIP5 ensemble (Table 2), (ii) the nine-member GCM ensemble that has been downscaled and (iii) the 18-member RCM ensemble (Table 1). Unfilled circles are CMIP5 GCMs listed in Table 2 that have not been downscaled. Filled circles represent GCMs that have been downscaled and these are connected by a line to the RCM(s) that have been used for downscaling. The vertical line represents the global mean warming at SWL1.5 and SWL2 relative to the control period (1971–2000).

tions in RCA4 compared to a range of other GCMs it has downscaled, indicating that the hydrological cycle is more sensitive to the increasing temperatures in this RCM. It is also noted that HadGEM2-ES has a very strong increase in SSTs over the Baltic Sea, as indicated by the local maxima in near-surface warming (not shown). Large SST changes in this region have previously been shown to have a very strong impact on regional climate modelling results (e.g. Kjellström and Ruosteenoja, 2007). As coarse-scale GCMs have a fairly poor representation of the Baltic Sea, care should be taken when analysing results from these models and preferably a coupled regional climate model system should be used (Kjellström et al., 2005). Apparently, many of the RCM simulations assessed here show larger precipitation increases (or smaller decreases) compared to the underlying GCMs for the Scandinavian domain, as also indicated by the ensemble mean statistics.

For eastern Europe Fig. 9 shows that simulated changes in temperature are slightly larger in summer than in winter at both SWLs. Also, the spread is larger in summer as a number of models give very strong temperature increases (among these are HadGEM2-ES that has been downscaled by the RCMs). For precipitation the simulations reveal an uncertainty not just in amplitude but also in sign of change in both winter and summer, with models indicating either increase or decrease. The ensemble mean shows a tendency towards a drying with less precipitation in summer, especially in SWL2. However, more than half of the GCMs and RCMs actually show increasing precipitation and it is clear that the ensemble average is heavily influenced by a smaller number of models with relatively strong decreases. Furthermore, several of these models also show a strong warming, indicating a feedback mechanism including reduced soil moisture. As for Scandinavia the spread becomes larger at SWL2 com-

pared to SWL1.5 and again we note that the RCM-simulated changes in temperature and precipitation mostly lie within the range of those as simulated by the underlying GCMs and by the larger CMIP5 ensemble. However, there are differences, of which the most notable is that none of the RCMs give a strong drying and warming in this region. This is even the case for the three RCMs downscaling HadGEM2-ES. Clearly, the RCMs change the summertime climate change signal in this region in a significant way resulting in both a smaller signal and less spread than that seen in the GCMs.

Summary statistics for the ensembles including minimum, maximum, SD and mean values for the regions in Fig. 1 are shown in Table 4. The numbers reveal that the three ensembles are different for both temperature and precipitation. Evidently, the smaller nine-member ensemble of GCMs that have been downscaled show less spread between the minimum and maximum compared to the larger 31-member CMIP5 ensemble from where they are taken. However, we note that the difference in spread as defined by 1 SD is relatively small and the intervals always overlap. A systematic difference is that the ensemble mean temperature increases are lower in the nine-member GCM subset compared to the full CMIP5 ensemble by between 0.06 and 0.29 °C for all eight regions in DJF or JJA. For SWL2 the same is found with corresponding differences in the range of 0.14–0.36 °C. These differences seem to be caused by a number of GCMs with a relatively strong response that has not been downscaled by any RCM (see Fig. 9). For precipitation we cannot find any similar systematic differences. Rather, the subset sometimes simulates wetter (or less dry) future conditions and sometimes the opposite.

Next we compare the RCM-simulated climate change signal with that of the underlying nine-member GCMs. Again, we note that the ensembles differ. While the fraction of European land with a consistent and robust change in precipitation is similar in the RCMs and the GCMs in winter, the RCMs give a considerably smaller fraction in summer (Table 3). Also, for wind speed there are differences between RCMs and GCMs in this respect. From Fig. 9 we see that the RCMs tend to give smaller increases in temperature and larger increases in precipitation (or less drying) than the GCMs. The differences in temperature ranges are most pronounced on the warmer side, with a substantially lower maximum warming in both summer and winter. The smaller spread among the ensemble members for the RCM simulations when it comes to temperature can also be seen in terms of lower SD. That the RCMs are modifying the climate change results compared to the underlying GCMs is also found in Keuler et al. (2016) and Sørland et al. (2018). Despite these changes we still note that in all seasons and all regions, the ranges given by the ensemble means plus or minus 1 SD overlap each other for both temperature and precipitation in all regions and for all seasons.

The results presented here indicate that (i) the RCM changes the climate change signal compared to the GCMs

they have been downscaling, (ii) the RCM ensemble is within the range of the wider CMIP5 ensemble for seasonal mean temperature and precipitation on the regional level, (iii) a different sampling of the CMIP5 ensemble would lead to different results in the resulting RCM ensemble with, implications on experimental design for impact studies.

5 Conclusions

The results show that simulated changes in temperatures indicate that Europe will warm in all seasons in the future and that these increases in temperature are highly consistent and robust over the ensemble despite considerable natural variability in the climate. Consequently, already at the SWL1.5, we note increasing temperature in all European areas in the vast majority of the simulations. The simulated temperature changes in Europe are mostly larger than the global mean warming. This is most pronounced in northern and northeastern Europe in winter and in southernmost and northernmost Europe in summer where warming is strongest. In these areas future temperature changes with respect to 1971–2000 are larger than, respectively, +1.5 and +2 °C at SWL1.5 and SWL2, which corresponds to a warming of almost +2 or +2.5 °C compared to pre-industrial (1861–1890) conditions.

The results indicate that precipitation will increase in most of Europe on an annual mean basis although with larger uncertainty than in temperatures. The current findings support earlier findings of more pronounced increases in all of Europe in winter and increases only in the north in summer when large parts of southern Europe are simulated to obtain less precipitation. At SWL1.5 changes are still relatively small with a spread among simulations that encompass zero change. At SWL2 larger, more consistent and robust changes are seen in both winter and summer.

Consistent patterns of changing wind speed are only found over parts of the Atlantic region where wind speed tends to decrease. Here we note that there is only little (if any) coherence between different simulations and it stands clear that future changes in wind speed are highly uncertain. Naturally, there is a strong impact of changes in the MSLP (i.e. large-scale circulation) on regional wind changes. We also find strong regional or local changes in some other areas, most notably oceanic areas in the north including the Arctic Ocean and parts of the Baltic Sea. We speculate that the wind speed increases in these areas are related to decreases in sea ice extent with consequent changes in stability conditions in the planetary boundary layer.

Changes in MSLP not only influence wind speed but also modify the climate change signal in temperature and precipitation. Examples of this include (i) changes in precipitation across the Scandinavian mountains with increases along the western side in connection to a stronger north–south MSLP gradient over the northern Atlantic in the northern part of the

model domain and vice versa and (ii) modifications of the warming signal with lower-than-average warming in southern Europe in simulations in which the storm tracks are displaced towards the north.

We note that the RCMs can alter the results of the GCMs, leading to either amplification or attenuation of the climate change signal in the underlying GCMs. For the EURO-CORDEX ensemble it is clear that the RCMs tend to produce less warming and more precipitation (or less drying) compared to the underlying GCMs in many areas in both winter and summer. The temperature results indicate that the RCM ensemble reduces the spread compared to the underlying GCMs. Furthermore, the chosen subset of GCMs gives a slightly weaker increase in temperature compared to that of the larger full CMIP5 ensemble. In particular, the subset has relatively fewer members showing strong warming in the region. Despite this we conclude that the spread represented by the SDs in the ensembles does overlap for all regions and seasons for both near-surface temperature and precipitation.

Data availability. The main web page documenting data availability for EURO-CORDEX data can be found at <http://euro-cordex.net/060378/index.php.en> (EURO-CORDEX community, 2018). In general all CMIP5 and EURO-CORDEX simulations that have been analysed here are accessible via the international Earth System Grid Federation (ESGF). HadCRUT4 data analysed for global mean temperature changes were downloaded at https://www.metoffice.gov.uk/hadobs/hadcrut4/data/current/time_series/HadCRUT4.6.0.0.annual_ns_avg.txt (Met Office Hadley Centre, 2018).

The Supplement related to this article is available online at <https://doi.org/10.5194/esd-9-459-2018-supplement>.

Competing interests. The authors declare that they have no conflict of interest.

Special issue statement. This article is part of the special issue “The Earth system at a global warming of 1.5 °C and 2.0 °C”. It is not associated with a conference.

Acknowledgements. Part of the work was carried out in the European Union Seventh Framework Programme in projects IMPACT2C under grant agreement 282746 and HELIX under grant agreement 603864. Part of this work was performed within the Swedish research program MSB-HazardSupport. We acknowledge the World Climate Research Programme’s Working Group on Coupled Modelling, which is responsible for CMIP, and we thank the climate modelling groups (listed in Table 2 of this paper) for producing and making their model output available.

For CMIP the US Department of Energy’s Program for Climate Model Diagnosis and Intercomparison provide coordinating support and led development of software infrastructure in partnership with the Global Organization for Earth System Science Portals.

Edited by: Zhenghui Xie

Reviewed by: two anonymous referees

References

- Aalbers, E. E., Lenderink, G., van Meijgaard, E., and van den Hurk, B. J. J.: Local-scale changes in mean and heavy precipitation in Western Europe, climate change or internal variability? *Clim. Dynam.*, <https://doi.org/10.1007/s00382-017-3901-9>, 2017.
- Alfieri, L., Burek, P., Feyen, L., and Forzieri, G.: Global warming increases the frequency of river floods in Europe, *Hydrol. Earth Syst. Sci.*, 19, 2247–2260, <https://doi.org/10.5194/hess-19-2247-2015>, 2015.
- Bador, M., Terray, L., Boé J., Somot, S., Alias, A., Gibelin, A.-L., and Dubuisson, B.: Future summer mega-heatwave and record-breaking temperatures in a warmer France climate, *Environ. Res. Lett.*, 12, 074025, <https://doi.org/10.1088/1748-9326/aa751c>, 2017.
- Bärring, L. and Strandberg, G.: Does the projected pathway to global warming targets matter?, *Environ. Res. Lett.*, 13, 024029, <https://doi.org/10.1088/1748-9326/aa9f72>, 2018.
- Christensen, J. H. and Christensen, O. B.: A summary of the PRUDENCE model projections of changes in European climate by the end of the century, *Clim. Change*, 81(1, Suppl.), 7–30, 2007.
- Christensen, O. B., Christensen, J. H., Machenhauer, B., and Botzet, M.: Very high-resolution regional climate simulations over Scandinavia – Present climate, *J. Climate*, 11, 3204–3229, 1998.
- Christensen, J. H., Kjellström, E., Giorgi, F., Lenderink, G., and Rummukainen, M.: Weight assignment in regional climate models, *Clim. Res.*, 44, 179–194, 2010.
- Colin, J., Déqué M., Radu, R., and Somot, S.: Sensitivity study of heavy precipitations in Limited Area Model climate simulation: influence of the size of the domain and the use of the spectral nudging technique, *Tellus A*, 62, 591–604, <https://doi.org/10.1111/j.1600-0870.2010.00467.x>, 2010.
- Déqué, M., Rowell, D. P., Lüthi, D., Giorgi, F., Christensen, J. H., Rockel, B., Jacob, D., Kjellström, E., de Castro, M., and van den Hurk, B.: An intercomparison of regional climate simulations for Europe: assessing uncertainties in model projections, *Clim. Change*, 81(1, Suppl.), 53–70, <https://doi.org/10007/s10584-006-9228-x>, 2007.
- Déqué, M., Somot, S., Sanchez-Gomez, E., Goodess, C. M., Jacob, D., Lenderink, G., and Christensen, O. B.: The spread amongst ENSEMBLES regional scenarios: regional climate models, driving general circulation models and inter annual variability, *Clim. Dynam.*, 38, 951–964, 2012.
- Deser, C., Phillips, A., Bourdette, V., and Teng, H.: Uncertainty in climate change projections: the role of internal variability, *Clim. Dynam.*, 38, 527–546, 2012.
- Donnelly, C., Greuell, W., Andersson, J., Gerten, D., Pisacane, G., Roudier, P., and Ludwig, F.: Impacts of climate change on

- European hydrology at 1.5, 2 and 3 degrees mean global warming above preindustrial level, *Clim. Change*, 143, 13–26, <https://doi.org/10.1007/s10584-017-1971-7>, 2017.
- EURO-CORDEX community: EUR-11, available at: <http://euro-cordex.net/060378/index.php.en>, last access: 10 March 2018.
- Fischer, E. and Knutti, R.: Anthropogenic contributions to global occurrence of heavy-precipitation and high-temperature extremes, *Nat. Clim. Change*, 5, 560–564, 2015.
- Frei, P., Kotlarski, S., Liniger, M. A., and Schär, C.: Future snowfall in the Alps: projections based on the EURO-CORDEX regional climate models, *The Cryosphere*, 12, 1–24, <https://doi.org/10.5194/tc-12-1-2018>, 2018.
- Giorgi, F. and Bi, X.: Time of emergence (TOE) of GHG-forced precipitation change hot-spots, *Geophys. Res. Lett.*, 36, L06709, <https://doi.org/10.1029/2009GL037593>, 2009.
- Gutowski Jr., W. J., Giorgi, F., Timbal, B., Frigon, A., Jacob, D., Kang, H.-S., Raghavan, K., Lee, B., Lennard, C., Nikulin, G., O'Rourke, E., Rixen, M., Solman, S., Stephenson, T., and Tangang, F.: WCRP COordinated Regional Downscaling EXperiment (CORDEX): a diagnostic MIP for CMIP6, *Geosci. Model Dev.*, 9, 4087–4095, <https://doi.org/10.5194/gmd-9-4087-2016>, 2016.
- Hawkins, E. and Sutton, R.: The potential to narrow uncertainty in regional climate predictions, *B. Am. Meteorol. Soc.*, 90, 1095–1107, 2009.
- Hawkins, E. and Sutton, R.: Time of emergence of climate signals, *Geophys. Res. Lett.*, 39, L01702, <https://doi.org/10.1029/2011GL050087>, 2012.
- Hawkins, E., Ortega, P., Suckling, E., Schurer, A., Hegerl, G., Jones, P., Joshi, M., Osborn, T., Masson-Delmotte, V., Mignot, J., Thorne, P., and van Oldenborgh, G.: Estimating changes in global temperature since the pre-industrial period, *B. Am. Meteorol. Soc.*, 98, 1841–1856, <https://doi.org/10.1175/BAMS-D-16-0007.1>, 2017.
- IPCC: Summary for policymakers, In: *Climate Change 2014: Impacts, Adaptation, and Vulnerability. Part A: Global and Sectoral Aspects. Contribution of Working Group II to the Fifth Assessment Report of the Intergovernmental Panel on Climate Change*, edited by: Field, C. B., Barros, V. R., Dokken, D. J., Mach, K. J., Mastrandrea, M. D., Bilir, T. E., Chatterjee, M., Ebi, K. L., Estrada, Y. O., Genova, R. C., Girma, B., Kissel, E. S., Levy, A. N., MacCracken, S., Mastrandrea, P. R., and White, L. L., Cambridge University Press, Cambridge, UK and New York, NY, USA, 1–32, 2014.
- Jacob, D., Elizalde, A., Haensler, A., Hagemann, S., Kumar, P., Podzun, R., Rechic, D., Remedio, A., R., Saeed, F., Sieck, K., Teichmann, C., and Wilhelm, C.: Assessing the transferability of the regional climate model REMO to different coordinated regional climate downscaling experiment (CORDEX) regions, *Atmosphere*, 3, 181–199, <https://doi.org/10.3390/atmos3010181>, 2012.
- Jacob, D., Petersen, J., Eggert, B., Alias, A., Christensen, O. B., Bouwer, L. M., Braun, A., Colette, A., Déqué, M., Georgievski, G., Georgopoulou, E., Gobiet, A., Menut, L., Nikulin, G., Haensler, A., Hempelmann, N., Jones, C., Keuler, K., Kovats, S., Kröner, N., Kotlarski, S., Kriegsmann, A., Martin, E., van Meijgaard, E., Moseley, C., Pfeifer, S., Preuschmann, S., Radermacher, C., Radtke, K., Rechid, D., Rounsevell, M., Samuelsson, P., Somot, S., Soussana, J.-F., Teichmann, C., Valentini, R., Vautard, R., Weber, B., and Yiou, P.: EURO-CORDEX: new high-resolution climate change projections for European impact research, *Reg. Environ. Change*, 14, 563–578, 2014.
- Jones, C., Giorgi, F., and Asrar, G.: The Coordinated Regional Downscaling Experiment: CORDEX, An international downscaling link to CMIP5, *CLIVAR Exchanges*, 56, 34–40, 2011.
- Keuler, K., Radtke, K., Kotlarski, S., and Lüthi, D.: Regional climate change over Europe in COSMO-CLM: Influence of emission scenario and driving global model, *Meteorol. Z.*, 25, 121–136, <https://doi.org/10.1127/metz/2016/0662>, 2016.
- King, A. D. and Karoly, D. J.: Climate extremes in Europe at 1.5 and 2 degrees of global warming, *Environ. Res. Lett.*, 12, 114031, <https://doi.org/10.1088/1748-9326/aa8e2c>, 2017.
- Kjellström, E. and Ruosteenoja, K.: Present-day and future precipitation in the Baltic Sea region as simulated in a suite of regional climate models, *Clim. Change*, 81, 281–291, 2007.
- Kjellström, E., Döscher, R., and Meier, H. E. M.: Atmospheric response to different sea surface temperatures in the Baltic Sea: Coupled versus uncoupled regional climate model experiments, *Nord. Hydrol.*, 36, 397–409, 2005.
- Kjellström, E., Nikulin, G., Hansson, U., Strandberg, G., and Ullerstig, A.: 21st century changes in the European climate: uncertainties derived from an ensemble of regional climate model simulations, *Tellus A*, 63, 24–40, 2011.
- Kjellström, E., Thejll, P., Rummukainen, M., Christensen, J. H., Boberg, F., Christensen, O. B., and Maule, C. F.: Emerging regional climate change signals for Europe under varying large-scale circulation conditions, *Clim. Res.*, 56, 103–119, <https://doi.org/10.3354/cr01146>, 2013.
- Kjellström, E., Bärring, L., Nikulin, G., Nilsson, C., Persson, G., and Strandberg, G.: Production and use of regional climate model projections – a Swedish perspective on building climate services, *Clim. Serv.*, 2–3, 15–29, <https://doi.org/10.1016/j.cliser.2016.06.004>, 2016.
- Knist, S., Goergen, K., Buonomo, E., Christensen, O. B., Colette, A., Cardoso, R. M., Fealy, R., Fernández, J., García-Díez, M., Jacob, D., Kartsios, S., Katragkou, E., Keuler, K., Mayer, S., van Meijgaard, E., Nikulin, G., Soares, P. M. M., Sobolowski, S., Szepszo, G., Teichmann, C., Vautard, R., Warrach-Sagi, K., Wulfmeyer, V., and Simmer, C.: Land–atmosphere coupling in EURO-CORDEX evaluation experiments, *J. Geophys. Res.-Atmos.*, 122, 79–103, <https://doi.org/10.1002/2016JD025476>, 2016.
- Kotlarski, S., Keuler, K., Christensen, O. B., Colette, A., Déqué, M., Gobiet, A., Goergen, K., Jacob, D., Lüthi, D., van Meijgaard, E., Nikulin, G., Schär, C., Teichmann, C., Vautard, R., Warrach-Sagi, K., and Wulfmeyer, V.: Regional climate modeling on European scales: a joint standard evaluation of the EURO-CORDEX RCM ensemble, *Geosci. Model Dev.*, 7, 1297–1333, <https://doi.org/10.5194/gmd-7-1297-2014>, 2014.
- Maule, C. F., Mendlik, T., and Christensen, O. B.: The effect of the pathway to a two degrees warmer world on the regional temperature change of Europe, *Clim. Serv.*, 7, 3–11, <https://doi.org/10.1016/j.cliser.2016.07.002>, 2017.
- Met Office Hadley Centre: HadCRUT4.6.0.0 Global (NH+SH)/2 Annual, available at: <https://www.metoffice.gov.uk/hadobs/>

- hadcrut4/data/current/time_series/HadCRUT.4.6.0.0.annual_ns_avg.txt, last access: 18 March 2018.
- Mitchell, D., James, R., Forster, P. M., Betts, R. A., Shiogama, H., and Allen, M.: Realizing the impacts of a 1.5 °C warmer world, *Nat. Clim. Change*, 6, 735–737, <https://doi.org/10.1038/nclimate3055>, 2016.
- Morice, C. P., Kennedy, J. J., Rayner, N. A., and Jones, P. D.: Quantifying uncertainties in global and regional temperature change using an ensemble of observational estimates: The HadCRUT4 dataset, *J. Geophys. Res.*, 117, D08101, <https://doi.org/10.1029/2011JD017187>, 2012.
- Moss, R. H., Edmonds, J. A., Hibbard, K. A., Manning, M. R., Rose, S. K., van Vuuren D. P., Carter, T. R., Emori, S., Kainuma, M., Kram, T., Meehl, G. A., Mitchell, J. F. B., Nakicenovic, N., Riahi, K., Smith, S. J., Stouffer, R. J., Thomson, A. M., Weyant, J. P., and Wilbanks, T. J.: The next generation of scenarios for climate change research and assessment, *Nature*, 463, 747–756, <https://doi.org/10.1038/nature08823>, 2010.
- Nikulin, G., Lennard, C., Dosio, A., Kjellström, E., Chen, Y., Hänsler, A., Kupiainen, M., Laprise, R., Mariotti, L., Fox Maule, C., van Meijgaard, E., Panitz, H.-J., Scinocca, J., and Somot, S.: The effects of 1.5 and 2 degrees of global warming on Africa in the CORDEX ensemble, *Environ. Res. Lett.*, <https://doi.org/10.1088/1748-9326/aab1b1>, in press, 2018.
- Prein, A. F., Gobiet, A., Truehett, H., Keuler, K., Goergen, K., Teichmann, C., Fox Maule, C., van Meijgaard, E., Déqué, M., Nikulin, G., Vautard, R., Colette, A., Kjellström, E., and Jacob, D.: Precipitation in the EURO-CORDEX 0.11° and 0.44° simulations: high resolution, high benefits? *Clim. Dynam.*, 46, 383–412, <https://doi.org/10.1007/s00382-015-2589-y>, 2016.
- Rockel, B. and Woth, K.: Extremes of near-surface wind speed over Europe and their future changes as estimated from an ensemble of RCM simulations, *Clim. Change*, 81, 267–280, 2007.
- Rummukainen, M.: State-of-the-art with regional climate models, *WIREs Clim. Change*, 1, 82–96, 2010.
- Schleussner, C.-F., Lissner, T. K., Fischer, E. M., Wohland, J., Perrette, M., Golly, A., Rogelj, J., Childers, K., Schewe, J., Frieler, K., Mengel, M., Hare, W., and Schaeffer, M.: Differential climate impacts for policy-relevant limits to global warming: the case of 1.5 °C and 2 °C, *Earth Syst. Dynam.*, 7, 327–351, <https://doi.org/10.5194/esd-7-327-2016>, 2016.
- Schurer, A. P., Mann, M. E., Hawkins, E., Tett, S. F. B., and Hegerl, G. C.: Importance of the pre-industrial baseline for likelihood of exceeding Paris goals, *Nat. Clim. Change*, 7, 563–567, 2017.
- Skamarock, W. C., Klemp, J. B., Dudhia, J., Gill, D. O., Duda, D. M. B. M. G., Huang, X.-Y., Wang, W., and Powers, J. G.: A description of the advanced research WRF version 3, NCAR Technical note 475, National Centre for Atmospheric Research, Boulder, Colorado, USA, 2008.
- Smiatek, G., Kunstmann, H., and Senatore, A.: EURO-CORDEX regional climate model analysis for the Greater Alpine Region: Performance and expected future change, *J. Geophys. Res.-Atmos.*, 121, 7710–7728, 2016.
- Sørland, S. L., Schär, C., Lüthi, D., and Kjellström, E.: Regional climate models reduce biases of global models and project smaller European summer warming, *Environ. Res. Lett.*, submitted, 2018.
- Taylor, K. E., Stouffer, R. J., and Meehl, G. A.: An Overview of CMIP5 and the Experiment Design, *B. Am. Meteorol. Soc.*, 93, 485–498, <https://doi.org/10.1175/BAMS-D-11-00094.1>, 2012.
- Tobin, I., Jerez, S., Vautard, R., Thais, F., Déqué, M., Kotlarski, S., Fox Maule, C., van Meijgaard, E., Nikulin, G., Noel, T., Prein, A., and Teichmann, C.: Climate change impacts on the power generation potential of a European mid-century wind farms scenario, *Environ. Res. Lett.*, 11, 034013, 2016.
- UNFCCC: The Paris Agreement. United Nations Framework Convention on Climate Change, available at: http://unfccc.int/paris_agreement/items/9485.php (last access: 10 March 2018), 2015.
- van der Linden, P. and Mitchell, J. F. B. (Eds.): ENSEMBLES: climate change and its impacts: summary of research and results from the ENSEMBLES project, Met Office Hadley Centre, Exeter, UK, 160 pp., 2009.
- van Meijgaard, E., Van Ulft, L. H., Lenderink, G., de Roode, S. R., Wipfler, L., Boers, R., and Timmermans, R. M. A.: Refinement and application of a regional atmospheric model for climate scenario calculations of Western Europe, Climate changes Spatial Planning publication: KvR 054/12, the Programme Office Climate changes Spatial Planning, Nieuwegein, the Netherlands, ISBN/EAN 978-90-8815-046-3, 44 pp. 2012.
- van Ulden, A. P. and van Oldenborgh, G. J.: Large-scale atmospheric circulation biases and changes in global climate model simulations and their importance for climate change in Central Europe, *Atmos. Chem. Phys.*, 6, 863–881, <https://doi.org/10.5194/acp-6-863-2006>, 2006.
- Vautard, R., Gobiet, A., Sobolowski, S., Kjellström, E., Stegehuis, A., Watkiss, P., Mendlik, T., Landgren, O., Nikulin, G., Teichmann, C., and Jacob, D.: The European climate under a 2 °C global warming, *Environ. Res. Lett.*, 9, 034006, <https://doi.org/10.1088/1748-9326/9/3/034006>, 2014.
- WMO: WMO Statement on the Status of the Global Climate in 2016, WMO-No. 1189, ISBN 978-92-63-11189-0, Geneva, Switzerland, 2017.